

Numerical Simulation of Entropy Generation in Hydrogen-Air Burner

Souad Morsli^{1*}, Amina Sabeur¹ and Mohammed El Ganaoui²

Abstract The aim of this work is the numerical simulation of the combustion of hydrogen with air in a burner and the numerical solution of local entropy generation rate in the combustion chamber. The effects of equivalence ratio ϕ and oxygen percentage γ on combustion and entropy generation rates are studied for different ϕ (ranging from 0 to 1.0) and γ values (ranging from 10 to 30%). The predictions show that the increase of ϕ (or the decrease of λ) reduces notably the reaction rate levels. The equations of continuity, of energy and momentum are solved by volume finite using commercial code CFD Fluent, the effects of turbulence will be modeled by the RNG-K-epsilon model, on the other hand the generation of the entropy will be introduced in post-processing.

Keywords: Combustion, entropy generation, CFD Fluent, RNG-K-epsilon.

1 Introduction

Combustion is defined as the burning of a fuel and oxidant to produce heat and/or work. It is the major energy which releases mechanism in the Earth and key to humankind's existence. Combustion includes thermal, hydrodynamic, and chemical processes. It starts with the mixing of fuel and oxidant, and sometimes in the presence of other species or catalysts. The fuel can be gaseous, liquid, or solid and the mixture may be ignited with a heat source. When ignited, chemical reactions of fuel and oxidant take place and the heat releases from the reaction creates self-sustained process.

Turbulent combustion of hydrocarbon fuels and the incineration of various industrial by products and wastes are an integral part of many segments of the chemical process and power industries.

Research into transport phenomena in energy systems and applications has substantially increased during the past a few decades due to its diversity in applications. This makes the special issue a most timely addition to existing literature. It includes recent major developments in both the fundamental and applications, and provides a valuable source to researchers dealing with analysis of entropy generation in thermal systems and processes.

Second law of thermodynamics states that all real processes are irreversible. Entropy

¹ University of Science and Technology Mohamed BOUDIAF of Oran, Laboratoire des Sciences et Ingénierie Maritimes, Algeria.

² University of Lorraine, IUT / LERMAB-Longwy, 186 rue de Lorraine, 54400 Cosne et Romain France.

Email: souad.morsli@univ-usto.dz

* Corresponding author. Tel.: +213 794643004; E-mail: Morsli.souad@yahoo.fr

generation is a measure of the amount of irreversibility associated with the real processes. As entropy generation takes place, the quality of energy (the exergy) decreases. This is a reality in any fluid flow process. In order to preserve the quality of energy in a fluid flow process or at least to reduce the entropy generation, it is important to study the distribution of the entropy generation within the fluid volume.

Therefore, in recent years, entropy minimization has become a topic of great interest in the thermo-fluid area. Bejan [A. Bejan(1980), A. Bejan(1996)] has spent much effort to determine the gap between thermodynamics, heat transfer, and fluid mechanics. He has applied the second law of thermodynamics to determine the entropy generations due to heat and flow transport and consequently minimize the entropy generation. Many studies are also carried on second law analysis and the entropy generation due to the heat transfer and fluid friction in duct flows under various conditions by several authors such as: Mahmud *et al* [S. Mahmud, R.A.Fraser(2003)], Sahin [A.Z. Sahin(1999)], [A.Z.Sahin(2000)], Yilbas *et al* [S.Z.Shuja, B.S. Yilbas, M.O.Budair(2001)], Shuja *et al* [B.S.Yilbas, S.Z.Shuja, M.Rashid(2003)], Demirel *et al* [Y.Demirel, R.Kahraman(1999)]. However, the combustion of hydrogen and various hydrocarbon fuels with air in a burner were considered by Yapici [H. Yapici, N. Kayatas, B. Albayrak, G. Basturk(2005)] to determine numerically the local entropy generation rate in the combustion chamber. The effect of the equivalence ratio on the combustion and entropy generation rate were also investigated. Dongyue *et al*. [J.Dongyue, Y. Wenming, C. KianJon(2013)] investigated the effects of heat recuperation on entropy generation in micro-cylindrical combustors. Their study was based on a complete analysis involving detailed simulations of H₂ /air premixed flame. An experimental validation was also performed to verify the numerical simulation results. Chen *et al*. [S. Chen, H. Han, Z. Liu, J. Li, C. Zheng(2010)] studied the entropy generation in counter-flow combustion. They observed that the entropy generation due to chemical reaction was predominant as Reynolds number was smaller than 60 while the largest share of entropy generation came from fluid friction when Reynolds number was larger than 100. Briones [A. Briones, A. Mukhopadhyay, SK. Aggarwal(2009)] investigated the entropy generation in hydrogen-enriched co-flow Methane-air propagating triple flames. One of the important finding was that the H₂ addition to methane fuel was increased, the integrated entropy generation increased primarily due to enhanced heat conduction and chemical reactivity but the second law efficiency of the system remains nearly constant with H₂ addition. Nishida *et al*. [K. Nishida, T. Takagi, S. Kinoshita(2002)] analyzed the entropy generation and exergy loss in both premixed and diffusion flames. The effects of equivalence ratio, fuel type and swirl ratio on the entropy generation rate were evaluated numerically. A comprehensive account of entropy analysis in combustion systems is available in the review by Som and Datta [SK. Soma, A. Datta(2008)].

This work considers the combustion of hydrogen with air due to the high temperature and velocity gradients in combustion chamber using a single burner element. In order to investigate the effect of oxygen percentage and entropy generation rate. Therefore, CFD codes can serve as a powerful tool used to perform low cost parametric. The results are in good agreement with the previous works [H Yapici, G Basturk, N Kayatas, B. Albayrak(2006)].

2 Mathematical model

The model considered in this study is assumed as two-dimensional and axisymmetric. The configuration of the geometry is indicated in Figure 1. The fuel and air inlets are coaxial and incorporate downstream. The model used for the numerical calculations include the RNG(renormalization group theory) k-ε for turbulent flow however for chemical species transport and reacting flow, the eddy-dissipation model with the diffusion energy source option is adopted. The mixture (hydrogen-air) is assumed as an ideal gas; no-slip conditions are assumed at the burner element walls.

2.1 Governing equations

The mass conservation equation and species transport is defined:

$$\frac{\partial \rho}{\partial t} + \frac{\partial \rho u_i}{\partial x_i} = 0 \quad (1)$$

And the mass conservation equation for k species is written as follows:

$$\frac{\partial \rho Y_k}{\partial t} + \frac{\partial}{\partial x_i} \left(\rho (u_i + v_{k,j}) Y_k \right) = \dot{\omega}_k \text{ For } k = 1, N \quad (2)$$

The momentum conservation equation is also defined as:

$$\frac{\partial}{\partial t} \rho u_j + \frac{\partial}{\partial x_i} \rho u_i u_j = -\frac{\partial P}{\partial x_i} + \frac{\partial \tau_{i,j}}{\partial x_i} + \rho \sum_{k=1}^N Y_k f_{k,j} = \frac{\partial \sigma_{ij}}{\partial x_i} + \rho \sum_{k=1}^N Y_k f_{k,j} \quad (3)$$

and

$$\tau_{ij} = -\frac{2}{3} \mu \frac{\partial u_k}{\partial x_k} \delta_{ij} + \mu \left(\frac{\partial u_i}{\partial x_j} + \frac{\partial u_j}{\partial x_i} \right) \quad (4)$$

The energy conservation equation is written as follows:

$$\frac{\partial \rho H_s}{\partial t} + \frac{\partial}{\partial x_i} (\rho u_i h_s) = \dot{\omega}_T + \dot{Q} + \frac{DP}{Dt} + \frac{\partial}{\partial x_i} \left(\lambda \frac{\partial T}{\partial x_i} \right) + \tau_{ij} \frac{\partial u_j}{\partial x_i} - \frac{\partial}{\partial x_i} \left(\rho \sum_{k=1}^N V_{k,i} Y_k h_{s,k} \right) \quad (5)$$

The equations for the RNG k-ε turbulence model – The turbulence kinetic energy, k, and the dissipation rate, ε, are determined using the following transport equations, respectively:

$$\frac{\partial}{\partial x_i} (\rho x_i k) = \frac{\partial}{\partial x_i} (\alpha_k \mu_{eff} \frac{\partial k}{\partial x_i}) + G_k - \rho \epsilon \quad (6)$$

$$\frac{\partial}{\partial x_i} (\rho x_i \epsilon) = \frac{\partial}{\partial x_i} (\alpha_\epsilon \mu_{eff} \frac{\partial \epsilon}{\partial x_i}) + \frac{\epsilon}{k} (C_{1\epsilon} G_k - C_{2\epsilon} \rho \epsilon - \chi)$$

The eddy dissipation model, introduced by Magnussen and Hjertager [BF. Magnussen, BH. Hjertager(1976)] is given by the expressions below:

$$R_{i,r} = v_{i,r}' W_{\omega,i} A \rho \frac{\epsilon}{k} \min_R \left(\frac{Y_R}{v_{R,r}' W_{\omega,R}} \right) \quad (7)$$

$$R_{i,r} = v_{i,r}' W_{\omega,i} A B \rho \frac{\varepsilon}{k} \left(\frac{\sum p Y_p}{\sum_J v_{j,r}'' W_{\omega,j}} \right)$$

The set of equations is completed by writing boundary conditions

At the fuel inlet ($x = 0$ and $0 < r < r_f$), $u_x = U_f$, $U_r = 0$, and $T = T_{in}$

At the air inlet ($x = 0$ and $r_i < r < r_0$), $u_x = U_{air}$, $u_r = 0$, $T = T_{in}$

At the isolated walls ($x = 0$, $r_i < r < r_0$ and $r_0 < r < R$), $\partial T / \partial x = 0$ $U_r = 0$ (8)

At the burner wall ($r = R$, and $0 < x \leq L$)

Stoichiometric Hydrogen air mixture was considered and its chemical kinetics was modeled with a one-step reaction mechanism ($N_R=1$ and species number $N=3$).The reaction mechanism takes place according to the constraints of chemistry, in a classical way:



3 Entropy generation rate:

When both temperature and velocity fields are known, the volumetric entropy generation rate s_{gen}''' at each point in the system can be calculated as follows (Bejan [1]),

$$s_{gen}''' = (s_{gen}''')_{heat} + (s_{gen}''')_{fric} \quad (10)$$

Where $(s_{gen}''')_{heat}$ and $(s_{gen}''')_{fric}$ represent the entropy generation rates due to heat transfer and fluid friction, respectively, and are defined as:

$$(s_{gen}''')_{heat} = \frac{\lambda_{eff}}{T^2} \cdot \left[\left(\frac{\partial T}{\partial x} \right)^2 + \left(\frac{\partial T}{\partial r} \right)^2 \right] \quad (11)$$

$$\text{And } (s_{gen}''')_{fric} = \frac{\mu_{eff}}{T} \cdot \Phi$$

where Φ is

$$\Phi = 2 \cdot \left[\left(\frac{\partial u_x}{\partial x} \right)^2 + \left(\frac{\partial u_r}{\partial r} \right)^2 + \left(\frac{u_r}{r} \right)^2 \right] + \left(\frac{\partial u_x}{\partial r} + \frac{\partial u_r}{\partial x} \right)^2 \quad (12)$$

The total entropy generation rate over the volume \dot{s}_{gen} can be calculated as follows:

$$\dot{s}_{gen} = \oint s_{gen}''' \partial \theta \cdot \partial r \cdot \partial x \quad (13)$$

Bejan number, Be , which compares the magnitude of entropy generation due to heat transfer with the magnitude of the total entropy generation, is defined by:

$$Be = (\dot{S}_{gen})_{heat} / \dot{S}_{gen} \quad (14)$$

When $Be \gg 0.5$, irreversibility due to heat transfer dominates, while for $Be \ll 0.5$ the irreversibility due to viscous effects dominates. For $Be \cong 0.5$, entropy generation due to heat transfer is almost of the same magnitude as that due to fluid friction.

4 Computational tools

4.1 Grid independency test:

A grid independency study is performed to ensure grid independence of the

calculated results. Therefore a grid orientation giving the grid independent results was taken into account, so 300 x 50 cells in the axial direction and 250 x 50 cells in the radial direction was undertaken. The grid distributions are uniform within each region. Furthermore to this total cell number, 100 axial lines were added in order to have more accuracy in the temperature and velocity derivatives calculations.

4.2 Numerical procedure

Model equations were implemented in the commercial CFD software FLUENT 6.3.26 [Fluent Inc] and appropriate user defined functions were incorporated for post processing the numerical solution to obtain data on entropy generation. The model selected to solving conservation equations describing convection, diffusion, and reaction sources for each component is the mixing and transport of chemical species.

The RNG $k - \epsilon$ model was used as a turbulence model in this study. The simulation values are resumed in table 1. While the inlet velocities of air and stoichiometric air/fuel ratios are presented in table 2. In order to achieve higher-order accuracy at cell faces, second-order upwind scheme was selected.

5 Results and discussion

Figure 3 shows the contours of reaction rates in the combustion chamber for the cases of $\phi = 0.5$ and 1.0 , and oxygen percentage in air $\gamma = 10$ and 30% respectively. The effect of reactions is apparent from these figures. It was clearly seen that with the increase of γ these regions contract in the axial direction however they expand in the radial direction. So, the reaction rate decreases significantly with the increase of ϕ .

The mass fraction of species H_2O in the combustion chamber, are plotted in figure 4 for $\phi = 0.5, 1$ and $\gamma = 10\%, 30\%$. The results obtained from this figure show that in the cases of $\phi < 1$, complete combustion occurs (all hydrogen molecules are completely burned into H_2O molecules). while in the case of $\phi = 1$ it is very close to the complete combustion state.

Knowing that the heat, which is released in the chemical reaction and transferred into the flowing gas including the reactant and product molecules, increases the temperature of this gas. In order to view the temperature distribution, 2-D temperature distributions within the burner in the cases of $\phi = 0.5, 1$ and $\gamma = 10\%, 30\%$ are counteracted in figure 5. It is very important to notice that the increase of ϕ significantly reduces the gradients so, larger temperature gradients occur in the axial direction (especially between $x = 0$ and about 0.20 m). The heat calculations performed for the each fuel case bring out that in the case of $\phi < 1$, the total heat per unit mass released in the combustion,

Consequently, the results obtained from this figures show that in the cases of $\phi < 1$, complete combustion occurs, while in the case of $\phi = 1$ it is very close to the complete combustion state.

Figure 6 presents the volumetric local entropy generation rate for $\phi = 0.5$ and $\gamma = 30\%$ and $\phi = 1$ and $\gamma = 10\%, 30\%$ plotted as the logarithmic contours; high entropy is generated in the region, in which the reaction rates are effective, and in which the large positive and negative temperature gradients occur in the axial and radial directions. The maximum values of volumetric local entropy generation rates vary in the range of (5.93 as the logarithmic) to (6.22 as the logarithmic) depending ϕ and γ .

It is apparent from that figure that the variations of ϕ and γ have an irregular effect on the volumetric local entropy generation rate distribution. These values bring out that the volumetric local entropy generation rates decrease in the cases of $\phi = 0.5$ and 1.0 respectively, with an increase of γ from 10 to 30%.

Figure 7 shows the Bejan number contours, it was clearly seen that (Be), is very close to 1 and this, therefore, means that the irreversibility due to the heat transfer dominates; it's due to the lower value of the entropy generation rates due to the fluid friction respect to those due to the heat transfer.

6 Conclusions

The combustion of hydrogen with air in a burner was inspected in order to simulate numerically the local entropy generation rate. The concluding remarks bring out that the increase of ϕ reduces notably the reaction rate levels, however, in the case of $\phi < 1$ and $\phi = 1$, the complete combustion arises and the combustion was very close to the complete combustion state respectively. The total entropy generation rates seem to decrease with increasing equivalent ratio and oxygen percentage in air. It was also noticed that the Bejan number is beside to 1 in all investigated cases. Thus, the irreversibility due to the heat transfer dominates. Due to the high temperature and for reducing the burner-wall temperature, the heat transfer coefficient at the burner wall should be increased.

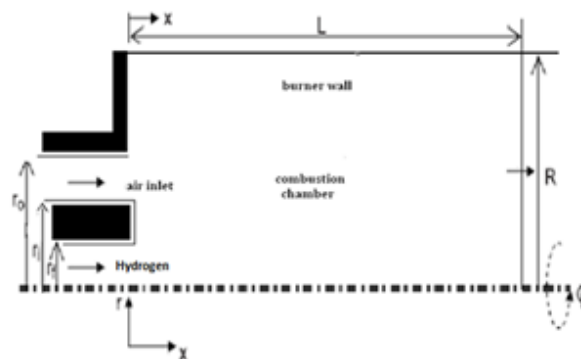


Figure1: Geometry of the burner

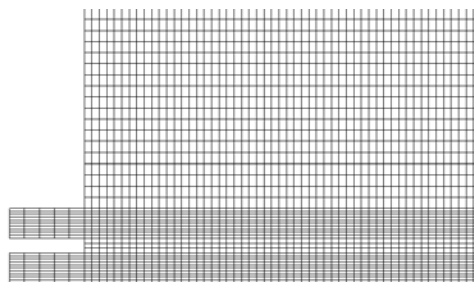


Figure2: Grid of the geometry

- Contours of reactions rates

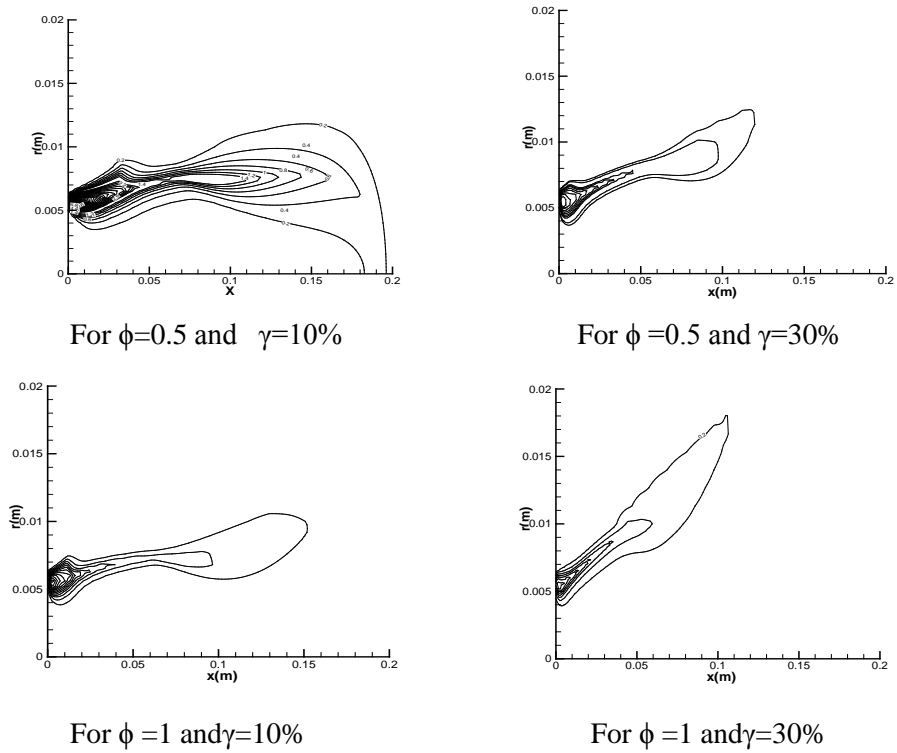


Figure 3: Contours of reactions rates for different values of equivalence ratio and oxygen percentage in air γ

• Mass fractions

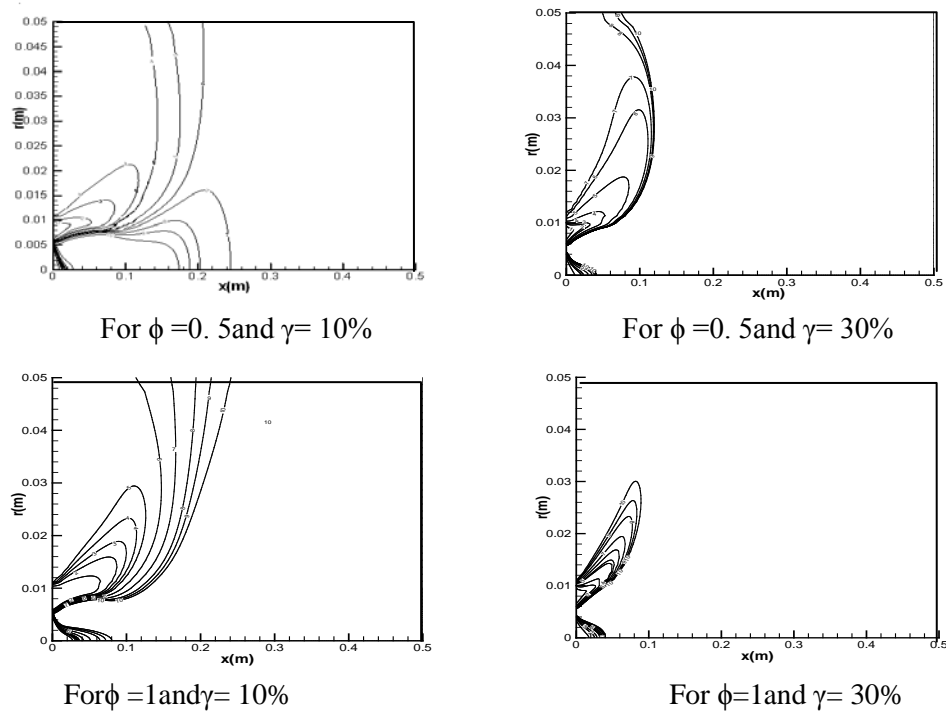
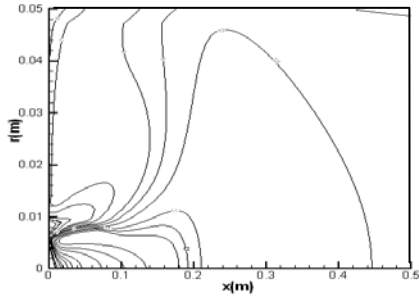
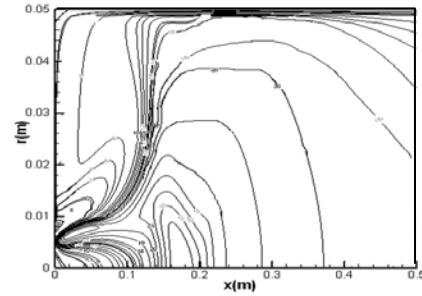


Figure 4: Mass fractions of species $\phi=0.5, 1$ and $\gamma =10\%, 30\%$

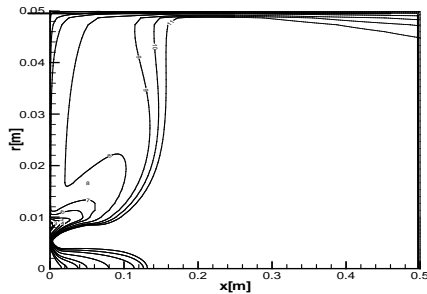
• **Temperature distribution**



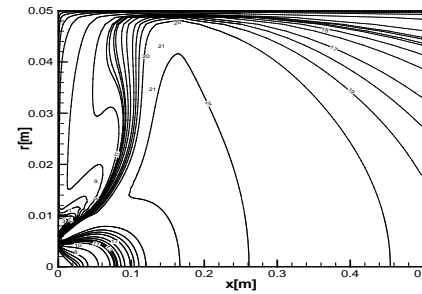
For $\phi=0.5$ and $\gamma=10\%$



For $\phi=0.5$ and $\gamma=30\%$



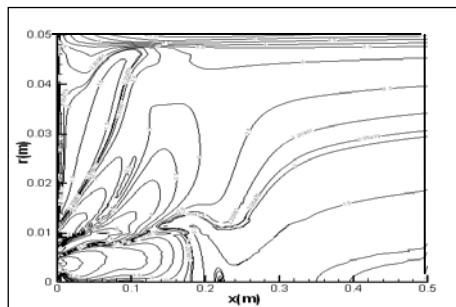
For $\phi=1$ and $\gamma=10\%$.



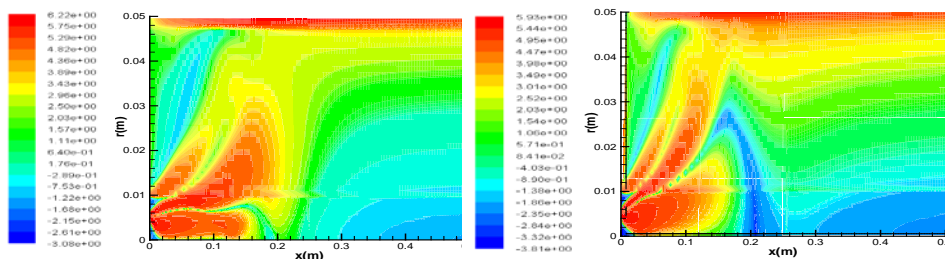
For $\phi=1$ et $\gamma=30\%$

Figure 5: Temperature distribution for $\phi = 0.5, 1.0$ and $\gamma=10\%; 30\%$

• **Entropy generation**



For $\phi =0.5$ and $\gamma=30\%$



For $\phi = 1$ and $\gamma = 10\%$

For $\phi = 1$ and $\gamma = 30\%$

Figure 6: Logarithmic volumetric local entropy generation rate contours.

• **Bejan number**

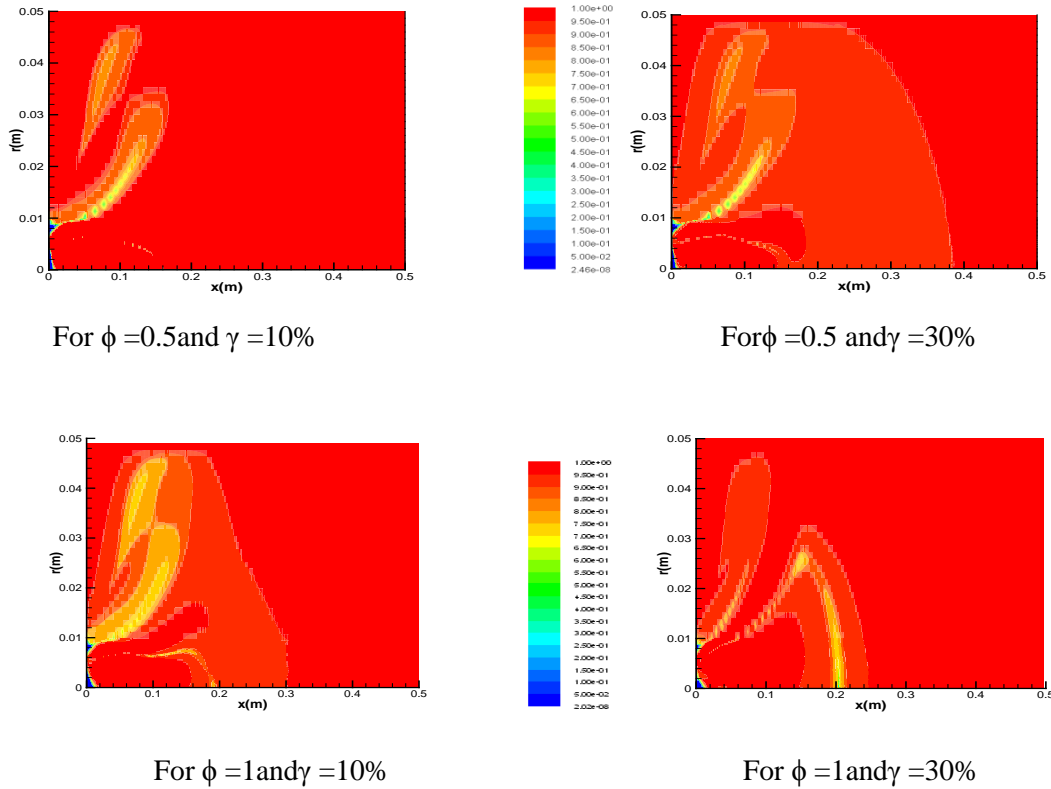


Figure7: Bejan Number Contours

Acknowledgment : The first author acknowledge his training period in the University of Lorraine (IUT of Longwy) permitting the achievement of the present work.

References

A. Bejan. (1980) Second law analysis in heat transfer, Energy 5 (8–9) 721–732.

A. Bejan. (1996) Entropy generation minimization, CRC Press, Boca Raton, Fl.

A.Z. Sahin. (1999) Effect of variable viscosity on the entropy generation and pumping power in a laminar fluid flow through a duct subjected to constant heat flux. Heat Mass Transfer 35: 499–506.

A.Z.Sahin. (2000) Entropy generation in turbulent liquid flow through a smooth duct subjected to constant wall temperature. Int. J. Heat Mass Transfer. 43: 1469-1478.

A. Briones; A. Mukhopadhyay; SK. Aggarwal. (2009) Analysis of entropy

generation in hydrogen-enriched methane-air propagating triple flames. *International Journal of Hydrogen Energy*;34:1074e83.

B.S.Yilbas; S.Z.Shuja; M.Rashid. (2003) Confined swirling jet impingement onto an adiabatic wall. *Int.J. Heat Mass Transfer* 46: 2947–2955.

BF. Magnussen; BH. Hjertager. (1976) On mathematical models of turbulent combustion with special emphasis on soot formation and combustion. In: 16th Symp. (Int'l.) on combustion. The Combustion Institute..

H. Yapici; N. Kayatas; B. Albayrak; G. Basturk. (2005) Numerical study on local entropy generation in a burner fueled with various fuels. *Heat Mass Transfer*;41:519e34.

H Yapici; G Basturk; N Kayatas; B. Albayrak. (2006) Effect of oxygen fraction on local entropy generation in a hydrogen–air burner. *Heat Mass Transfer*;43:37–53. Fluent Inc. 2006 FLUENT 6.3.26 User's guide. (Fluent Inc).

J.Dongyue; Y. Wenming; C. KianJon. (2013) Entropy generation analysis of H₂/air premixed flame in micro-combustors with heat recuperation, *Chemical Engineering Science* 98265–272..

K. Nishida; T. Takagi; S. Kinoshita. (2002) Analysis of entropy generation and exergy loss during combustion. *Proc Combust Inst*;29:869e74.

S. Mahmud; R.A.Fraser. (2003) The second law analysis in fundamental convective heat transfer problems. *Int. J. Thermal Sci.* 42: 177–186.

S.Z.Shuja; B.S. Yilbas; M.O.Budair. (2001) Local entropy generation in an impinging jet: minimum entropy concept evaluating various turbulence models. *Comput.Methods Appl. Mech. Eng.* 190: 3623–3644.

S. Chen; H. Han; Z. Liu; J. Li; C. Zheng. (2010) Analysis of entropy generation in non-premixed hydrogen versus heated air counter-flow combustion. *Int.J.Hydrogen Energy*35, 4736–4746.

SK. Soma; A. Datta. (2008) Thermodynamic irreversibilities and exergy balance in combustion processes. *Prog Energy Combust Sci*;34:351e76.

Y.Demirel; R.Kahraman. (1999) Entropy generation in a rectangular packed duct with wall heat flux. *Int. J. Heat Mass Transfer* 42: 2337–2344.

Nomenclature

Latin symbols

CFD	Computational fluid dynamics
C_μ , $C_{\varepsilon 1}$, $C_{\varepsilon 2}$	Coefficients in $k-\varepsilon$ turbulence model
$f_{k,j}$	
H	Enthalpy
$h_{s,k}$	enthalpy of species
K	Turbulent kinetic energy
L	Length of burner
P	Pressure
Q	Heat transfer rate
R	Universal gas constant
RNG	Renormalization group
r	Radial distance
r_i	Inner radius of air inlet
r_0	Outer radius of air inlet
s'''_{gen}	Volumetric entropy generation rate
\dot{s}'''_{gen}	Integrated entropy generation rate

Greek symbols

δ_{kj}	Kronecker delta
ε	turbulent energy dissipation rate
ϕ	Equivalence ratio
Φ	Viscous dissipation
λ	Air excess ratio
γ	Oxygenpercentage in air
μ	Dynamic viscosity
ρ	Density
θ	Tangential direction
ρ_k	Density of the species k
σ_{ij}	Tensor of the constraint in plan i and the direction j
τ	Stress tensor
T_{ij}	Tensor of the viscous constraints
T	Temperature
Y_k	Mass fraction of the species k

Annexes

Table 1: Physical values of the simulation

r_f	0.004(m)
r_i	0.006(m)
r_0	0.01(m)
R	0.05(m)
L	0.5(m)
T	300(k)
h_{amb}	10 (W/m ² K)
P_{op}	101325 (Pa)
$\rho_{hydrogen}$	0.08189 (kg/m ³)
ρ_{air}	1.225 (kg/m ³)

Table 2: Inlet velocities of air and stoichiometric air/fuel ratios for $U_f=20.251(m/s)$ and $\dot{Q} = 10000(W)$

Uair (m/s)		
γ %	$\phi =0.5$	$\phi =1.0$
10	47.699	23.850
12	39.861	19.930
14	34.262	17.131
16	30.063	15.031
18	26.797	13.398
20	24.184	12.098
22	22.046	11.023
24	20.265	10.132
26	18.758	9.379
28	17.466	8.733
30	16.346	8.173